Anthrax Toxin Protective Antigen: Inhibition of Channel Function by Chloroquine and Related Compounds and Study of Binding Kinetics Using the Current Noise Analysis

Frank Orlik, Bettina Schiffler, and Roland Benz

Lehrstuhl für Biotechnologie, Theodor-Boveri-Institut (Biozentrum) der Universität Würzburg, Am Hubland, D-97074 Würzburg, Germany

ABSTRACT   Protective antigen (PA) of the tripartite anthrax toxin binds to a cell surface receptor and mediates the transport of two enzymatic components, edema factor and lethal factor, into the cytosol of host cells. Here recombinant PA_{63} from *Bacillus anthracis* was reconstituted into artificial lipid bilayer membranes and formed ion permeable channels. The heptameric PA_{63}-channel contains a binding site for 4-aminoquinolones, which block ion transport through PA in vitro. This result allowed a detailed investigation of ligand binding and the stability constants for the binding of chloroquine, fluphenazine, and quinacrine to the binding site inside the PA_{63}-channel were determined using titration experiments. Open PA_{63}-channels exhibit *1/f* noise in the frequency range between 1 and 100 Hz, whereas the spectral density of the ligand-induced current noise was of Lorentzian type. The analysis of the power density spectra allowed the evaluation of the on- and off-rate constants (k_1 and k_{-1}) of ligand binding. The on-rate constants of ligand binding were between 10^6 and 10^8 M^{-1} s^{-1} and were dependent on the ionic strength of the aqueous phase, sidedness of ligand addition, as well as the orientation and intensity of the applied electric field. The off-rates varied between $\sim$10 s^{-1} and 2600 s^{-1} and depended mainly on the structure of the ligand.

INTRODUCTION

The main virulence factors of *Bacillus anthracis* are the poly-D-glutamiccapsule, which inhibits phagocytosis, and anthrax toxin. The plasmid-encoded tripartite anthrax toxin comprises a receptor-binding moiety termed protective antigen (PA) and two enzymatically active components, edema factor (EF) and lethal factor (LF) (Friedlander, 1986; Mock and Fouet, 2001; Collier and Young, 2003). PA binds to cells, coordinates self-assembly of heptamers, and finally delivers EF and LF to the cytosol of the target cell. This translocation scheme is common to many so-called binary AB-toxin including anthrax-, C2-, and iota-toxin (Barth et al., 2002). EF is a calcium and calmodulin-dependent adenylate-cyclase (89 kDa) that causes a dramatic increase of intracellular cAMP level, upsetting water homeostasis and destroying the balance of intracellular signaling pathways. In addition, EF is believed to be responsible for the edema found in cutaneous anthrax (Mock and Fouet, 2001; Lacy and Collier, 2002; Dixon et al., 1999). The second enzymatic component, LF, is a highly specific zinc metalloprotease (90 kDa) that removes specifically the N-terminal tail of mitogen-activated protein kinase kinases (MAPKKs). This cleavage initiates still poorly understood mechanisms leading to subsequent cell death by apoptosis. The correlation between MAPKK cleavage and the LF-dependent inhibition of the release of proinflammatory mediators like nitric oxide, tumor necrosis factor-α, and

interleukin-1β is an actual subject of particular interest (Hanna et al., 1993; Menard et al., 1996; Pellizzari et al., 1999). The monomeric anthrax PA, is a cysteine-free 83-kDA protein that binds to a ubiquitously expressed integral membrane receptor (ATR) (Bradley et al., 2001). PA_{83} bound to ATR is processed by a furin-like protease to a 63-kDa protein PA_{63}. The resulting 20-kDa fragment PA_{20} dissociates from the receptor bound carboxy-terminal 63-kDa fragment and is released into the extracellular milieu. $PA_{(63)}$ then spontaneously oligomerizes into a heptamer (Petosa et al., 1997) and binds up to three molecules of EF and/or LF with high affinity ($K_d \sim$ 1 nM) (Cunningham et al., 2002; Escuyer and Collier, 1991; Elliott et al., 2000). The assembled toxic complexes are then endocytosed and directed to endosomes. There, low pH results in the translocation of EF and LF across the endosomal membrane. For all pore-forming A-B toxins, it is still not clear if the pore lumen was the translocation pathway for the enzymatic components, or if enzyme delivery occurred in the boundary region between PA and lipid. The enzymes exert their toxic activities in the cytosol. The primary structure of PA shows no hydrophobic stretches that could serve as potential membrane-spanning regions. Based on the crystal structure of the homoheptameric complex (Petosa et al., 1997) and the structure of the structurally related, mushroom-shaped channel of *Staphylococcus aureus* α-hemolysin also formed by a heptamer (Song et al., 1996), a hypothetical model has been proposed (see Fig. 1). In this model, formation of a β-barrel channel requires: a), the unfolding of a Greek-key motif (strands $2\beta_1$-$2\beta_4$) to form a β-hairpin, and b), the association of seven β-hairpins in the PA_{63} heptamer to form a 14-stranded, membrane-spanning β-barrel (Nassi et al.,
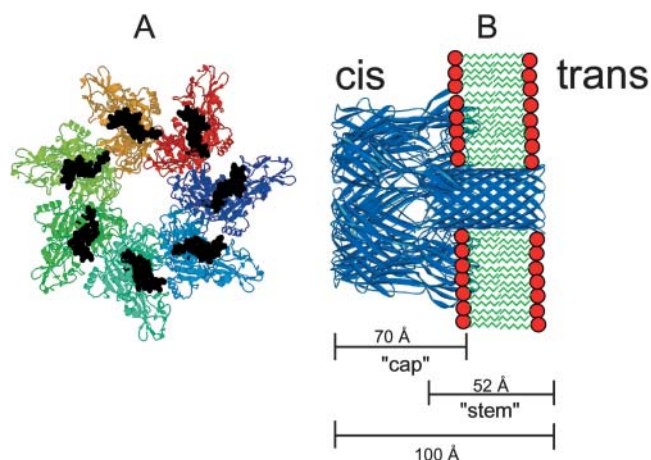
FIGURE 1 (*A*) Crystal structure of the water-soluble, heptameric ''prepore'' of PA. The structure of the membrane-spanning region has not been determined by x-ray crystallography and is indicated in black. (*B*) Model of the membrane inserted heptameric α-toxin of *S. aureus*.

2002). This conformational change is presumably induced by endosomal acidification, which may protonate histidines in the loop and key region of the heptameric PA_{63}-protein.

Addition of chloroquine and related compounds (see Fig. 2) led to a dose-dependent decrease of the PA-induced membrane conductance. This result suggested that PA heptamers contain a binding site for chloroquine inside the channel. On- and off-rate constants for compound binding to the PA-channel allowed a meaningful analysis of the structure function relationship of chloroquine binding to the PA-channel and the evaluation of the binding kinetics.

MATERIALS AND METHODS

Anthrax protective antigen PA_{63}

Recombinant, nicked anthrax protein $PA_{(63)}$ from *B. anthracis* was obtained from List Biological Laboratories (Campbell, CA). One milligram of lyophilized protein was dissolved in 1 ml 5-mM HEPES, 50 mM NaCl, pH 7.5, complemented with 1.25% trehalose. Aliquots were stored at $-20°C$.

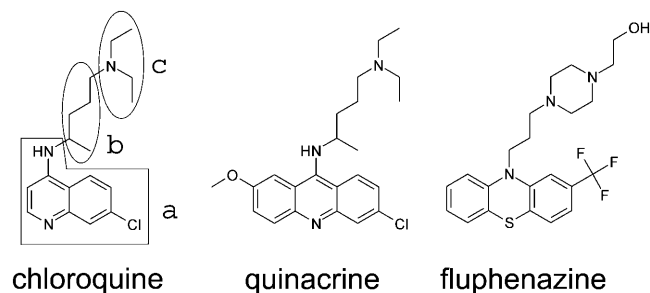FIGURE 2 Structures of chloroquine, quinacrine, and fluphenazine used in this study. For chloroquine the three subunits are indicated (*a*, *b*, and *c*).

Lipid bilayer experiments

Black lipid bilayer membranes were formed as described previously (Benz et al., 1978). The instrumentation consisted of a Teflon chamber with two aqueous compartments connected by a small circular hole. The hole had a surface area of ~ 0.4 mm^2. Membranes were formed by painting onto the hole a 1% solution of diphytanoyl phosphatidylcholine (Avanti Polar Lipids, Alabaster, AL) in *n*-decane. The aqueous salt solutions (Merck, Darmstadt, Germany) were buffered with 10 mM MES, pH 6. Control experiments revealed that the pH was stable during the time course of the experiments. Chloroquine and related compounds were obtained from Sigma (Deisenhofen, Germany). PA_{63} was reconstituted into the lipid bilayer membranes by adding concentrated stock solutions to the aqueous phase to one side (the *cis*-side) of a membrane in the black state. The temperature was kept at 20°C throughout.

Titration experiments

These measurements were performed with multichannel membranes. The membrane current was measured with a pair of Ag/AgCl electrodes with salt bridges switched in series with a battery-operated voltage source and a homemade current to voltage converter made using a Burr Brown (Dallas, TX) operational amplifier (with a three-pole filter). The feedback resistors of the current amplifier were between 0.01 and 10 GΩ. The amplified signal was recorded with a strip chart recorder to measure the absolute magnitude of the membrane current and to calculate the stability constant for ligand binding to PA. The conductance data of the titration experiments were analyzed using equations derived earlier for the carbohydrate-induced block of the maltoporin- and CymA-channels, respectively (Benz et al., 1987; Orlik et al., 2002, 2003).

Noise analysis

The amplified signal was simultaneously fed through a four-pole Butterworth low-pass filter (Krohn-Hite model 113340, Brockton, MA) into an AD-converting card of an IBM-compatible PC. The digitized data were analyzed with a homemade fast Fourier transformation program, which yielded identical results as compared to a commercial digital signal analyzer (Ono Sokki CF 210, Addison, IL). The spectra were composed of 400 points and they were averaged either 128 or 256 times. The power density spectra were analyzed using commercial graphic programs. For the derivation of the rate constants of ligand binding they were fitted to equations described in previously performed studies (Benz et al., 1987; Andersen et al., 1995; Orlik et al., 2002).

RESULTS

Single-channel conductance measurements

A receptor is involved in the binding and oligomerization of PA_{63} on the surface of mammalian cells (Escuyer and Collier, 1991). This is not required for reconstitution in artificial lipid bilayers, where channel activity is obtained under mildly acidic conditions (Blaustein et al., 1989). Recombinant PA_{63} was added while stirring from the concentrated stock solution (10 μg/ml) to the aqueous phase (concentration, ~ 10 ng/ml) bathing a black lipid bilayer membrane. The recombinant protein formed well-defined, cation-selective channels in lipid bilayer membranes, which exhibit rapid flickers especially at higher KCl concentrations (see Fig. 3). Its single-channel conductance of ~ 180 pS in 1 M KCl, 10 mM MES, pH 6 (applied voltage 50 mV) agrees
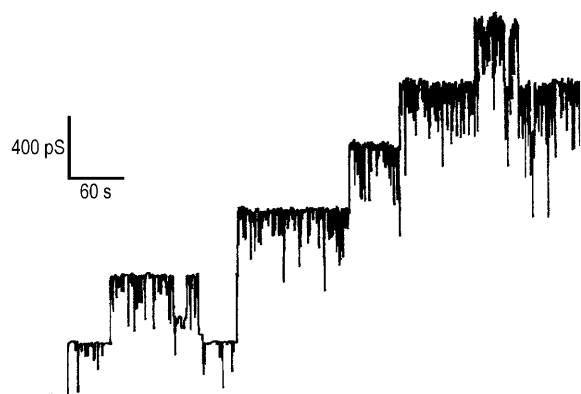
FIGURE 3 Single-channel recording of diphytanoyl phosphatidylcholine/ n-decane membranes in the presence of PA_{63}. The aqueous phase contained 3 M KCl, 10 mM MES (pH 6) and 10 ng/ml PA_{63}. The applied membrane potential was 20 mV; $T = 20°C$.

well with previous studies performed with trypsin nicked PA_{63} (Blaustein et al., 1989).

Charge effects of PA_{63} on ion transport

Table 1 shows a summary of the single-channel conductance of PA_{63} in different KCl concentrations. The data indicate that the single-channel conductance was not a linear function of the bulk aqueous KCl concentration. Instead a slope of ~0.5 was observed on a double-logarithmic scale for the conductance versus concentration curve (see Fig. 4). This result indicates that charge effects influence the properties of the PA_{63}-channel. These charge effects are caused by negatively charged groups either localized in the vestibule of the channel or in its inside resulting in a substantial ionic-strength dependent potential, which attracts cations and repels anions. A quantitative description of the effect of point charges on the single-channel conductance may be given by the following considerations. The first one is based on the Debeye-Hückel theory describing the effect of point charges in an aqueous environment. The second treatment was proposed by Nelson and McQuarrie (1975). In case of a negative point charge, q, in an aqueous environment a potential ϕ is created that is dependent on the distance, r, from the point charge:

FIGURE 4 Single-channel conductance of PA_{63} as a function the KCl concentration in the aqueous phase ($\bullet$). The solid line represents the fit of the single-channel conductance data with equation $G(c) = G_0 \times c_0^+$ assuming the presence of negative point charges (1.4 negative charges; $q = -2.24 \times 10^{-19}$ As) within the channel and assuming a channel diameter of 0.5 nm. c, concentration of the KCl solution in M (molar); G, average single-channel conductance in pico-Siemens (10^{-12} S); G_0, single-channel conductance in the absence of point negative charges given in pS/M. The dashed line shows the single-channel conductance of the PA_{63}-channel in the absence of point charges and corresponds to a linear function between channel conductance and bulk aqueous concentration; $G(c) = G_0 \times c$).

$$\Phi = \frac{q \times e^{-\frac{r}{l_D}}}{4\pi \times \varepsilon_0 \times \varepsilon \times r}. \quad (1)$$

ε_0 (= 8.85×10^{-12} F/m) and ε (= 80) are the absolute dielectric constants of vacuum and the relative constant of water, respectively, and l_D is the so-called Debeye length that controls the decay of the potential (and of the accumulated positively charged ions) in the aqueous phase:

$$l_D^2 = \frac{\varepsilon \times \varepsilon_0 \times R \times T}{2F^2 \times c}, \quad (2)$$

where c is the bulk aqueous salt concentration. The negative potential created by the negative point charge in the center of the channel has important implications on its ion transport properties. This effect of charges inside the channel has been predicted by Dani (1986) and Jordan (1987) for ion channels in general and has been experimentally verified in a Ca^{2+}-activated K^+-channel by chemical modification of surface carboxylate groups (MacKinnon et al., 1989).

Stability constants of substrate binding to PA_{63} under symmetric conditions

The binding component C2II of the binary actin ADP-ribosylating C2-toxin from *Clostridium botulinum* is structurally related to PA from *B. anthracis*. In previous studies (Bachmeyer et al., 2001, 2003), we demonstrated that the C2II-mediated ion current through lipid bilayer membranes could be blocked by the addition of 4-aminoquinolones. Here

TABLE 1 Single-channel conductance of PA_{63} in KCl solutions of different concentration c

KCl, c/M*	3	1	0.3	0.1	0.03
G/pS	400	180	120	70	40

*The membranes were formed of diphytanoyl phosphatidylcholine dissolved in n-decane. The aqueous solutions were buffered (10 mM MES, pH 6). The applied voltage was 50 mV, and the temperature was 20°C. The average single-channel conductance was calculated from at least 100 single events; c indicates the concentration of the aqueous KCl solution.
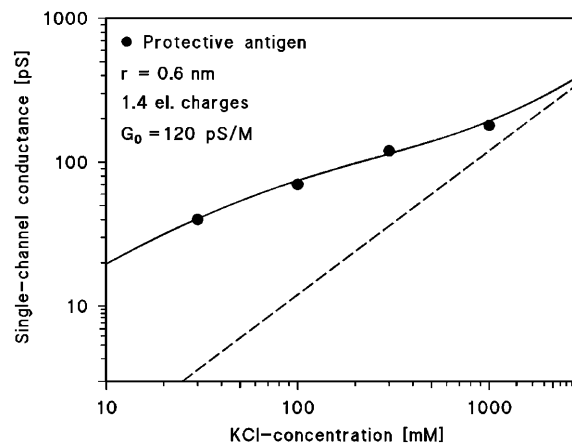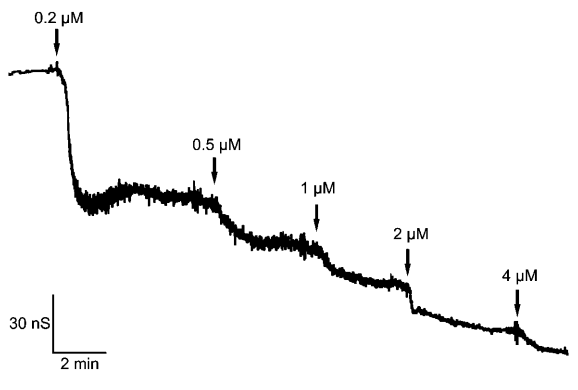
FIGURE 5　Titration of membrane conductance induced by PA_{63} with fluphenazine. The membrane was formed from diphytanoyl phosphatidyl-choline/n-decane. The aqueous phase contained 10 ng/ml protein (added only to one side of the membrane), 1 M KCl, and fluphenazine at the concentrations shown at the top of the figure. The temperature was 20°C and the applied voltage was 20 mV.

we report similar experiments with recombinant PA_{63}. An example for this type of measurements is shown in Fig. 5. After incorporation of 830 heptameric PA_{63}-channels in a lipid bilayer membrane increasing concentration of fluphenazine was added on both sides of the membrane to the aqueous phase (1 M KCl) while stirring to allow equilibration. The membrane current decreased in a dose-dependent manner. The titration curve given in Fig. 5 could be analyzed using a Lineweaver-Burke plot, which yielded a stability constant, K, of $\sim$2,250,000 M^{-1} (half-saturation constant $K_S = 0.44$ μM) for the binding of fluphenazine to the PA_{63}-channel in the experiment of Fig. 5 (see Fig. 6). Similar analyses were also performed in this study with chloroquine and quinacrine. Highest binding constants were found in 150 mM KCl solution for quinacrine ($K = 12,300,000$ 1/M) followed by fluphenazine ($K = 5,353,000$ 1/M) and chloroquine ($K = 675,600$ 1/M). The stability constants for
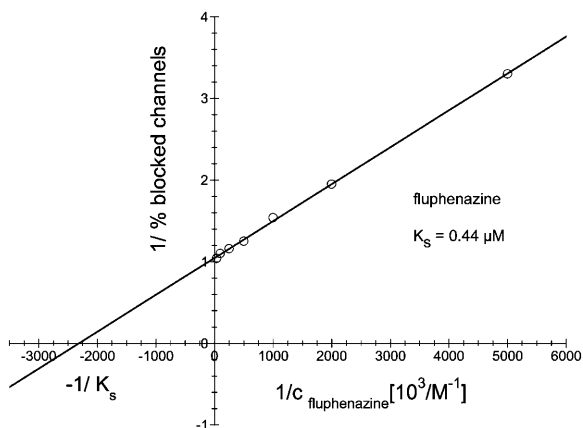

FIGURE 6　Lineweaver-Burke plot of the inhibition of the $PA_{(63)}$-induced membrane conductance by fluphenazine. The straight line corresponds to a stability constant K, for fluphenazine binding to PA_{63} of 2.25×10^6 l/mol ($K_S = 0.44$ μM).

4-aminoquinolones binding to PA_{63} are by a factor of $\sim$4 (fluphenazine) to 14 (quinacrine) higher than for C2-toxin (see Table 2).

Asymmetric ligand binding to the PA_{63}-channel

The channel forming heptameric PA_{63} is fully oriented in the lipid bilayer membranes (see Fig. 1) when it is added to only one side of the membrane (Blaustein et al., 1989). In accordance with previous binding experiments performed with C2II, the stability constant for chloroquine binding to the PA_{63}-channel was also found to be strongly asymmetric when the ligand was only added to the *cis*- or *trans*-side of the membrane (see Table 2). To check if asymmetry also exists for other ligands we also performed experiments with fluphenazine. The results are also included in Table 2. Like for C2II, we did not observe any asymmetry when fluphenazine was only added to the *cis*-side and the *trans*-side, respectively.

Analysis of the ligand-induced current noise through the PA_{63}-channel

Parallel to the titration measurements the spectral density was measured using fast Fourier transformation of the

TABLE 2　Stability constants K for the inhibition of channel formation by PA by chloroquine and related compounds in lipid bilayer membranes

Compound*	Side of addition	K / 10^3 M^{-1}	K^* / 10^3 M^{-1}(C2II)
		0.15 M KCl	
Chloroquine	Both sides	676	110
Quinacrine	Both sides	12,300	870
Fluphenazine	Both sides	5353	2100
		0.3 M KCl	
Chloroquine	Both sides	241	N.D.
Quinacrine	Both sides	3701	N.D.
Fluphenazine	Both sides	3626	N.D.
		1 M KCl	
Chloroquine	Both sides	55.2	22
	cis-side	56.3	16
	trans-side	1.9	4.7
Quinacrine	Both sides	740	166
Fluphenazine	Both sides	2100	620
	cis-side	909	300
	trans-side	842	810
		3 M KCl	
Chloroquine	Both sides	31.6	N.D.
Quinacrine	Both sides	890	322
Fluphenazine	Both sides	2000	N.D.

The data represent means of at least three individual titration experiments. The standard deviation was typically <10% of the mean value. The results of similar titration experiments performed with C2II toxin are given for comparison (K^*).

*The membranes were formed from diphytanoyl phosphatidylcholine/n-decane. The aqueous phase contained the indicated KCl and $\sim$10 ng/ml activated PA_{63}; $T = 20$°C. K^* values from C2II toxin are given for comparison and taken from Bachmeyer et al. (2003).
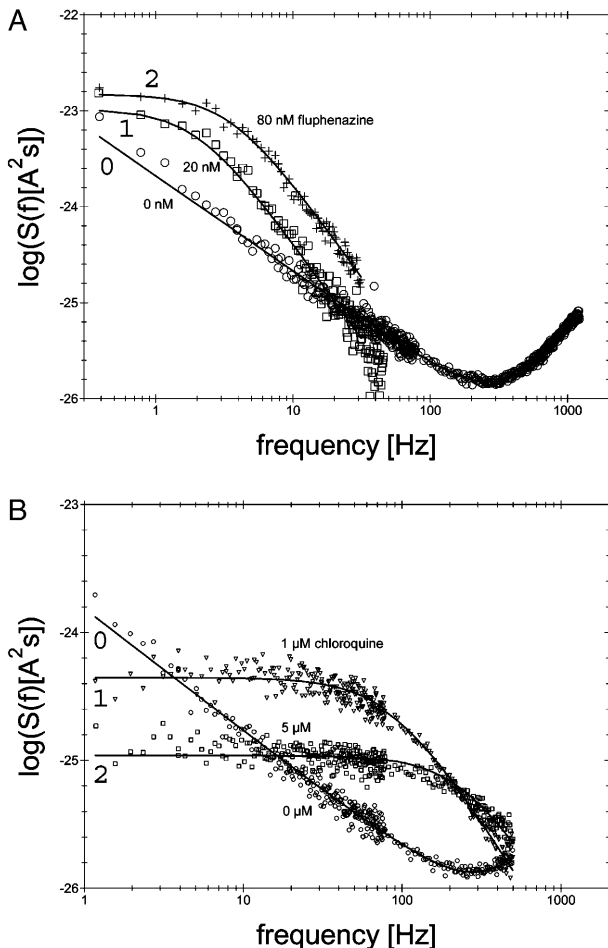
FIGURE 7 (A) Power density spectra of fluphenazine-induced current noise of ~1600 PA_{63}-channels (added only to the *cis*-side of the membrane). Trace 0 shows the control (150 mM KCl). (*Trace 1*) The aqueous phase contained 20 nM fluphenazine and the power density spectrum of trace 0 was subtracted ($\tau = 79.6$ ms; $S_0 = 10.43 \times 10^{-24}$ A^2s). (*Trace 2*) The aqueous phase contained 80 nM fluphenazine and the power density spectrum of trace 0 was subtracted ($\tau = 45.2$ ms; $S_0 = 14.9 \times 10^{-24}$ A^2s); $T = 20°C$; $V_m = 10$ mV. (B) Power density spectra of chloroquine-induced current noise of ~1400 PA_{63}-channels (added only to the *cis*-side of the membrane). Trace 0 shows the control (150 mM KCl). (*Trace 1*) The aqueous phase contained 1 μM chloroquine and the power density spectrum of Trace 0 was subtracted ($\tau = 1.77$ ms; $S_0 = 0.44 \times 10^{-24}$ A^2s). (*Trace 2*) The aqueous phase contained 5 μM chloroquine and the power density spectrum of trace 0 was subtracted ($\tau = 0.63$ ms; $S_0 = 0.11 \times 10^{-24}$ A^2s); $T = 20°C$; $V_m = 10$ mV.

current noise. After recording of reference spectra we added fluphenazine in increasing concentration to the aqueous phase with stirring to allow equilibration. An example is given in Fig. 7 A for the measurement of current noise of ~1600 PA_{63}-channels without fluphenazine (*trace 0*; 0 μM). At small frequencies up to ~100 Hz the spectral density was dependent on $1/f$, which is typical for open bacterial porin channels (Nekolla et al., 1994; Wohnsland and Benz, 1997; Bezrukov and Winterhalter, 2000). Trace 1 of Fig. 7 A shows a power density spectrum taken at 20 nM fluphenazine. In

further experiments the concentration of fluphenazine was increased in defined steps. At another concentration of fluphenazine ($c = 80$ nM) the power density spectrum corresponded to that of trace 2 in Fig. 7 A. The power density spectra of the current noise shown in Fig. 7 A (*traces 1* and *2*) corresponded to that of Lorentzian type and could be fitted to single Lorentzians after the subtraction of the reference spectrum.

The power density spectrum, $S(f)$, is given by a "Lorentzian" function:

$$S(f) = \frac{S_0}{1 + (f/f_c)^2}. \tag{3}$$

Such a type of noise is expected for a random switch with different on and off probabilities (Verveen and De Felice, 1974; De Felice, 1981; Conti and Wanke, 1975).

The corner frequencies, f_c, of the Lorentzians are dependent on the on- and off-rate constant, k_1 and k_{-1}, for fluphenazine binding to the binding site of the PA_{63}-channel. This means that the corner frequencies, f_c, should increase with increasing fluphenazine concentration.

Assuming small perturbations of the number of closed channels due to microscopic variations of the number of bound ligand molecules, the reaction rate of the second order reaction given in Eq. 3 is given by:

$$\frac{1}{\tau} = 2\pi \times f_c = k_1 \times c + k_{-1}. \tag{4}$$

This was the case for all noise measurements including the experiments shown in Fig. 7 A. The reaction rate $1/\tau$ was plotted as a function of the fluphenazine concentration in the aqueous phase. Fig. 8 shows the fit of the corner frequencies, f_c, of the experiments shown in Fig. 7 A and of other fluphenazine concentrations (data not shown). The rate constants for the binding of fluphenazine to the PA_{63}-

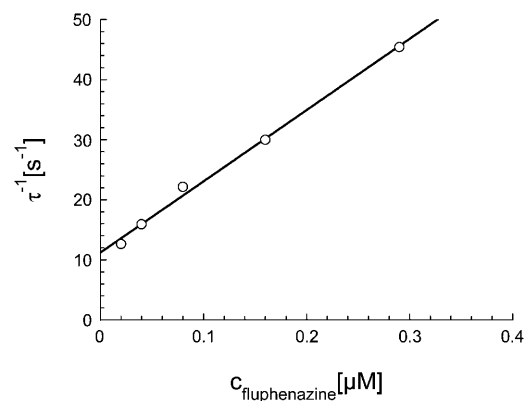FIGURE 8 Dependence of $2\pi f_c = 1/\tau$ on the fluphenazine concentration in the aqueous phase. The data were derived from the fit of the power density spectra with Lorentzians given in Fig. 7 A for fluphenazine concentrations ranging between 0.01 and 0.3 μM. The aqueous phase contained 150 mM KCl and 10 ng/ml PA added only to the *cis*-side of the membrane. The applied membrane potential was 20 mV; the temperature was 20°C.

channel were $k_1 = 119 \times 10^6$ $M^{-1} \cdot s^{-1}$ and $k_{-1} = 11.4$ s^{-1}. This corresponds to a stability constant, K, for the binding of fluphenazine to the binding site inside or at the PA_{63}-channel of 10,057,000 M^{-1}. Fig. 7 B shows a similar experiment performed with chloroquine. However, it is clear from the spectra of Fig. 7 B that the kinetics of chloroquine binding to PA_{63} is much faster than the kinetics of fluphenazine binding to PA_{63}. This reduces the plateau value S_0 of the power density spectra and also increases the corner frequency. Fitting of the corner frequencies similar to Fig. 8 (data not shown) resulted in the rate constants for the binding of chloroquine to the PA_{63}-channel: $k_1 = 350 \cdot 10^6$ $M^{-1} \times s^{-1}$ and $k_{-1} = 330 s^{-1}$. This corresponds to a stability constant, K, of 1,057,000 M^{-1}.

Table 3 shows the results of noise measurements performed with PA_{63} for different ligands and of noise measurements for chloroquine and fluphenazine added only to the *cis*-side or only to the *trans*-side of the membrane. The data suggest that only the on-rates are affected by the asymmetrical addition of the two ligands, whereas the off-rates are independent from the side of addition. This result may indicate that only one binding site exists at or in the PA_{63}-channel and that the ligands may permeate through PA_{63} to reach this binding site (see Discussion).

Effect of ionic strength on the ligand binding to the PA_{63}-channel

The binding of chloroquine and homologs to the PA_{63}-channel was dependent on the ionic strength as Table 2 clearly demonstrates. To study the effect of ionic strength on the binding of ligands to the PA_{63}-channel in some more detail we performed noise measurements at KCl concentrations of 1 M and 150 mM KCl, respectively. Table 3 shows that the on-rate constants increased with decreasing ionic strength, whereas the variation of the off-rate constant

did not seem to correlate with the KCl concentration. This means that the stability constant for binding of the 4-aminoquinolones to the PA_{63}-channel also increased considerably for decreasing ionic strength, indicating that ion-ion interactions between the positively charged ligand and negatively charged groups in or near the PA_{63}-channel lumen are responsible for the binding of the different ligands. This result clearly indicates that surface charge effects influence the binding properties of the ligands to the PA_{63}-channel. Accordingly, they influence the on-rate for ligand binding because their effective concentration is at low ionic strength much higher there than in the bulk aqueous phase (Bachmeyer et al., 2003)

Voltage-dependent asymmetric ligand binding

4-Aminoquinolones such as chloroquine are twofold positively charged at neutral pH. Therefore, binding of chloroquine to PA_{63} is supposed to be influenced by the polarity of the applied electric field. For all the measurements performed so far, we applied positive voltages to the *cis*-side of the membrane because the channels closed when negative voltages of more negative than -20 mV were applied to the *cis*-side. Table 4 summarizes the parameters of chloroquine-induced current noise in PA_{63} depending on the orientation and intensity of the applied electric field. The data show that both on- and off-rates were affected by the polarity of the applied electric field; even so the effect on k_1 was more pronounced. When chloroquine was added to the *trans*-side of the membrane and the applied voltage to the *cis*-side was negative (-20 mV), k_1 increased by a factor of 3.5 as compared to the opposite polarity of the electric field. Increasing positive voltages applied to the *cis*-side led to a strong decrease of the on-rate constant (k_1), whereas the off-rate constant (k_{-1}) remained essentially unaffected. At voltages $> +50$ mV no binding /translocation of chloroquine

TABLE 3 Parameters of ligand-induced current noise in PA_{63}

Compound*	Side of addition	k_1 / 10^6 $M^{-1} s^{-1}$	k_{-1} / s^{-1}	K / 10^3 M^{-1}
		1 M KCl		
Chloroquine	Both sides	42 ± 5 (74)	970 ± 163 (2600)	43.3
	cis-side	53 ± 3.3 (31)	900 ± 180 (1600)	61.8
	trans-side	1.5 ± 0.3 (9)	1020 ± 18 (1350)	1.43
Quinacrine	Both sides	13.7 ± 1.8 (34)	16.9 ± 4 (210)	850
Fluphenazine	Both sides	33.7 ± 2.2 (34)	14.1 ± 5.5 (55)	2770
	cis-side	10.7 ± 1.4 (17)	7.9 ± 2.2 (33)	1450
	trans-side	13.7 ± 1.6 (35)	8.6 ± 1.1 (45)	1640
		150 mM KCl		
Chloroquine	Both sides	363 ± 81 (140)	350 ± 24 (1600)	1030
Quinacrine	Both sides	128 ± 3.8 (120)	9.6 ± 2.5 (210)	14,120
Fluphenazine	Both sides	140 ± 30 (62)	10.1 ± 1 (44)	14,100

*The membranes were formed from diphytanoyl phosphatidylcholine/*n*-decane. The aqueous phase contained either 1 M or 150 mM KCl and ~10 ng/ml PA at the *cis*-side. k_1 and k_{-1} were derived from a fit of the corner frequencies as a function of the ligand concentration. K is the stability constant for ligand binding derived from the ratio k_1/k_{-1}. The data represent means ± SD of at least three individual experiments with the same ligand. Binding parameters of ligand binding to C2-toxin (in parentheses) are given for comparison.

TABLE 4 Parameters of chloroquine-induced current noise in PA$_{(63)}$ depending on the applied electric field

Side of ligand addition*	Voltage applied at the *cis*-side	$k_1 / 10^6$ M^{-1}s^{-1}	$k_{-1} / $ s^{-1}	$K / 10^3$ M^{-1}
		1 M KCl		
trans-side				
	+10 mV/−10 mV	1.7 / 3.3	826 / 1800	2.1 / 1.8
	+20 mV/−20 mV	1.2 / 5.3	720 / 2570	1.4 / 2.1
	+30 mV	0.42	690	0.61
	+40 mV	0.14	850	0.17
	+50 mV	0.04	990	0.04
	+60 mV	N.D.	N.D.	N.D.
	+70 mV	N.D.	N.D.	N.D.
cis-side				
	+10 mV	41	715	57
	+20 mV/−20 mV	54 / 35	730 / 1860	80 / 19
	+30 mV	65	760	86
	+40 mV	71	890	80
	+50 mV	74	960	77
	+60 mV	76	1200	64
	+70 mV	72	1420	51

*The membranes were formed from diphytanoyl phosphatidylcholine n-decane. The aqueous phase contained 1 M KCl and ~10 ng/ml PA$_{63}$ at the *cis*-side; $T = 20°$C. k_1 and k_{-1} were derived from a fit of the corner frequencies as a function of the ligand concentration. K is the stability constant for ligand binding derived from the ratio $k_1 k_{-1}$. The data represent mean of at least three individual experiments with the same ligand. The standard deviation was typically <10% of the mean value. N.D. means not detectable and indicates that the power density of the current noise could not be fitted to a Lorentzian function.

could be detected (see Table 4). In contrast, adding chloroquine to the *cis*-side, and applying positive voltages to the same side, resulted in increasing k_1 values, reaching a voltage independent plateau value at voltages >+50 mV. These data strongly argue for a voltage-dependent permeation of chloroquine through the PA-channel when it is added to the *cis*-side of the membrane. In addition, we could show that the asymmetric binding properties of chloroquine cannot be explained by the orientation of the applied electric field alone, because binding of chloroquine to PA$_{63}$ was clearly more asymmetric (factor of 40) than the effects created by the orientation of the applied electric field.

DISCUSSION

Stability constants for ligand binding to the PA$_{63}$-channel

In previous studies we already demonstrated that chloroquine and homologs bind to the binding component (C2II) of C2-toxin from *C. botulinum* and inhibit channel formation in vitro and intoxication in vivo at micromolar concentration (Bachmeyer et al., 2001, 2003). Protective antigen of anthrax toxin shares significant sequence identity (33%) with C2II, suggesting that the two proteins have similar modes of action. PA$_{63}$ has been crystallized in its monomeric and heptameric prepore form (Petosa et al., 1997; see Fig. 1). The

heptameric form is the one that binds to the target cell membrane and inserts a 14-stranded β-barrel into the membrane. The mushroom-shaped channel-forming complex of PA$_{63}$ is highly asymmetric, because most hydrophilic material is localized on one side of the membrane, the *cis*-side of lipid bilayer membranes or the surface of the target cell (see Fig. 1), and only a very small part of the oligomer is localized in the target cell membrane (Petosa et al., 1997). The structure is similar to that of α-toxin of *S. aureus*, which forms also a heptamer with some sort of vestibule on the *cis*-side (Song et al., 1996).

In this study we performed titration experiments with 4-aminoquinolones: chloroquine, quinacrine, and fluphenazine and found an even higher affinity of these compounds to PA$_{63}$ as compared to C2II (see Table 2). The affinity increased in the series chloroquine, quinacrine, and fluphenazine at 1 M KCl. The reduction of the ionic strength to more physiological conditions (150 mM), increased the stability constant further and the half saturation constant for quinacrine binding was ~81 nM under these conditions. The drastic increase of stability constants at low ionic strength might be caused by an interaction between oppositely charged groups localized at quinacrine and at PA$_{63}$, an interaction that is supposed to be ionic strength dependent. The strongest effect was observed for quinacrine; its stability constant increased by a factor of ~16 as compared to measurements performed in 1 M KCl.

It has to be noted that all of the substances listed above are commonly applied drugs and the concentrations used in our experiments are in a range that should allow therapeutical treatment to inhibit in vivo intoxication of cells by anthrax toxin. Quinacrine, for example, is used to treat giardiasis, a protozoal infection of the intestinal tract, and certain types of lupus erythematosus, an inflammatory disease that affects the joints, tendons, and other connective tissues and organs. Specific in vivo experiments for testing the inhibition of anthrax toxin-mediated intoxication of macrophage-like cells by 4-aminoquinolones are planned in future.

Evaluation of the stability constant of chloroquine binding to PA$_{63}$ under asymmetric conditions

Recombinant PA$_{63}$ reconstitutes into membranes in a fully oriented way as shown here and elsewhere (Blaustein and Finkelstein, 1990a). The channels are presumed to be heptameric ''mushrooms'', with an extracellular ''cap'' region and a membrane-inserted, β-barrel ''stem''. In artificial bilayer experiments the ''cap'' region is orientated to the *cis*-side of the membrane, the side where the protein was added. To investigate whether the binding of chloroquine to PA$_{63}$ was dependent on the orientation of the channel, we performed titration experiments where chloroquine and PA$_{63}$ were both added to the *cis*-side of the membrane. The stability constant for chloroquine binding to the *cis*-side of PA$_{63}$ was approximately the same as when it

was added to both sides of the membrane and a K of 56,300 1/M was obtained (1 M KCl). The addition of chloroquine to the *trans*-side of the membranes resulted in a drastic lower affinity for the PA$_{63}$-channel. In this case, K was ~1900 1/M in 1 M KCl. This means that the PA$_{63}$-channel exhibits considerable asymmetry for the binding of chloroquine. Interestingly, no significant asymmetry was detected for other 4-aminoquinolones like fluphenazine. Experiments in which the orientation of the applied electric field was varied, revealed a certain effect on chloroquine binding to PA$_{63}$, but could not explain the highly asymmetric binding of chloroquine to PA$_{63}$. It is noteworthy that it was impossible to study the voltage dependence of 4-aminoquinolone binding to PA for potentials more negative than −20 mV at the *cis*-side because of channel closure.

It has to be noted that similar experiments with symmetric tetraalkylammonium (TAA) ions have been performed by Blaustein et al. (Blaustein and Finkelstein, 1990a; Blaustein et al., 1990b). Symmetric quaternary ammonium ions block the PA-channel in a voltage-dependent fashion (at micromolar concentrations), when added to either the *cis*- or *trans*-compartment. The authors stated that TAA ions are permeable and driven through the channel by large voltages of the appropriate sign. These blockers were more potent from the *cis*-side because ~20-fold higher concentrations were needed on the *trans*-side to achieve comparable effects.

On- and off-rate constants for ligand binding to the PA-channel

Based on the titration experiments we suggested that channel block by the different ligands occurs in an association-dissociation reaction. Like porins of Gram-negative bacteria or channel-forming toxins (e.g., C2II from *C. botulinum*), the open PA$_{63}$-channels exhibit *1/f* noise that is probably related to the structure of the heptameric channel and may be caused by transient changes of the channel structure that is not controlled by a chemical reaction and has nothing to do with ligand binding (see Fig. 3) (Nekolla et al., 1994; Wohnsland and Benz, 1997; Bezrukov and Winterhalter, 2000). The addition of 4-aminoquinolones leads to a complete change of the spectral density $S(f)$ of current noise, which is given by a so-called Lorentzian function of the frequency f.

The analyses of the Lorentzians allow the evaluation of the rate constants and the stability constants for ligand binding to the PA$_{63}$-channel. The corner frequency f_c is a function of the ligand concentration, which allows the calculation of rate constants of binding to the site in or near the channel based on a simple chemical reaction for ligand binding. We did not observe any indication for the binding of more than one ligand molecule at the same time to the binding site, i.e., the occurrence of two Lorentzians. The existence of one binding site for symmetric TAA ions inside the PA$_{63}$-channel has been proposed by Blaustein et al. (Blaustein and Finkelstein, 1990a; Blaustein et al., 1990b). Blaustein and Finkelstein

(1990a) interpreted the diffusion-controlled binding of TAA to the PA$_{63}$-channel with a simple two-barrier, single-well model of the channel. We are therefore convinced that this simple model provides a good description of ligand binding to the PA$_{63}$-channel and of the blockage of the ion movement by their binding.

The core scaffold of 4-aminoquinolones can be divided into three different subunits (*a*, *b*, and *c*). There is a bicyclic (chloroquine) or tricyclic (quinacrine, fluphenazine) moiety (*a*) containing one or two heteroatoms and at least one substituent. This ring system is linked through an alkyl spacer (*b*) to a basic moiety (*c*) (see Fig. 2). Previous experiments clarified that for an adequate binding the positively charged ammonium group and the bulky ring system play an important role (Bachmeyer et al., 2003). The on-rate for the binding of the different ligands to the PA$_{63}$ was between 1.4×10^7 1/(M × s) and 4.2×10^7 1/(M × s) in 1 M KCl, which means that it did not vary much with the structures of the different ligands. When the ionic strength was decreased to 150 mM the on-rates were between 14×10^7 1/(M × s) and 36×10^7 1/(M × s) again exhibiting only minor differences. Obviously the ionic strength has a much higher effect on the on-rate of ligand binding than their structure. These results suggest that the high on-rate of binding for all ligands is already close to that of diffusion-controlled reaction processes (Eigen et al., 1964).

In contrast to the on-rate the off-rate of the binding of the different ligands showed much higher variations and increased from fluphenazine (14 s^{-1}) over quinacrine (17 s^{-1}) to chloroquine (971 s^{-1}). These data illustrate that for increasing size of the different ligands k_{-1} decreased. Highest off-rates were obtained with compounds that have only two conjugated aromatic rings at the side chain. From those with three conjugated aromatic rings fluphenazine with a trifluoromethyl group at the ring structure has the smallest off-rate in 1 M KCl. This means also that the ligands should be permeable through the channel, otherwise it cannot be understood why they block the channel from both sides. The asymmetry for chloroquine binding that was observed in experiments where it was only added to one side of the membrane may be explained by the assumption that the molecules diffusing through the channel can leave more easily the binding site on the *cis*-side of the channel because of the high off-rate. The membrane-spanning domain of PA comprises the residues E302–S325 with a conserved pattern of alternating hydrophobic and hydrophilic amino acids and a total quantity of three negatively charged residues orientated toward the channel lumen (E302, E308, and D315). Site-directed mutagenesis of negatively charged residues located in the membrane-spanning region did not show any significant effect on 4-aminoquinolones binding to the C2II-channel (Blöcker et al., 2003). In addition, recent investigations performed with cysteine mutants of PA revealed that upon binding of MTS-ET reagents to mutated PA binding of the positively charged channel blocker tetrabutyl ammonium

(TBA) from the *trans*-side of the protein is blocked. Nassi and co-workers (Nassi et al., 2002) demonstrated that after S349C mutant channels had reacted with MTS-ET, subsequent addition of TBA to the *cis*-side produced the usual 3.5-fold decrease in conductance, whereas the MTS-ET reaction prevented *trans*-TBA from producing its usual twofold decrease in conductance. This result suggested that the TBA binding site is located somewhere in the cap region of the PA_{63} protein.

To summarize we conclude, that, like for C2-toxin, the vestibule of the PA_{63} on the *cis*-side contains the negatively charged residues that are involved in binding of 4-amino-quinolones. Fluphenazine, which has a higher affinity to the binding site, has a much smaller off-rate, which means that the molecules diffusing through the channel are caught at the binding site in the vestibule, thus increasing the effective concentration at this point. The off-rate constants were only a little dependent on the ionic strength in the range between 150 mM and 1 M KCl. Only for the experiments with quinacrine in 150 mM KCl a substantial decrease of the off-rate (9.6 s^{-1}) was observed. This observation agrees well with measurements performed with C2II-toxin where a significant decrease of k_{-1} was only observed at 20 mM KCl (Bachmeyer et al., 2003) suggesting that ionic strength effects influence also the off-rate of ligand binding to a small extent (Blöcker et al., 2003).

Voltage-dependent block of PA-channels by chloroquine

Increasing positive voltages applied to the *cis* (chloroquine-containing) side of the membrane led to somewhat increasing on-rates, reaching a voltage-independent plateau value of $\sim74 \times 10^6$ $M^{-1}s^{-1}$ at $+50$ mV. This could be caused by diffusion limitation as pointed out above. These considerations support our view that the binding site for the 4-aminoquinolones is localized in the vestibule of the PA-channel.

In contrast, addition of chloroquine to the *trans*-side and application of high positive voltages to the *cis*-side, led to a decrease of on-rates and blocking of PA was abolished at positive voltages >50 mV. In this case, membrane voltage influenced both on-rate and stability constant of binding but not the off-rate, presumably because the compounds have to diffuse through the channel against the electric field to reach the binding site in the vestibule.

CONCLUSIONS

Inhibition of anthrax toxin

One key challenge in treating systemic anthrax is to inhibit the toxin action. To do so PA is certainly one of the main targets, because its channel-forming activity is essential for the uptake of the two enzymatic components into cells. The use of polyclonal antibodies against PA has been shown to give guinea pigs reasonable passive protection against anthrax infection (Little et al., 1997; Kobiler et al., 2002). In the past year, novel toxin inhibitors have been described. Many of these inhibitors are derivatives of a toxin component or of the receptor. One synthetic inhibitor was designed by selecting a peptide from a phage-display library that was able to compete with LF for its binding to the PA_{63} heptamer (Mourez et al., 2001). Multiple copies of this peptide were covalently linked to a flexible polyacrylamide backbone, resulting in a polyvalent molecule that could prevent intoxication of rats challenged with a combination of PA and LF, lethal toxin (LTx). Another interesting class of inhibitors represents dominant negative mutant forms of PA that specifically block pore formation and translocation. Rats challenged with purified LTx were protected when injected with dominant negative mutant forms of PA in which selected residues lining the pore lumen had been mutated (Sellman et al., 2001a). These mutated PA molecules were able to bind cells, oligomerize and bind LF but were unable to form channels and translocate the toxin complex (Sellman et al., 2001b).

In this study, we present a novel group of potent channel blockers, which can block the PA_{63}-channel in vitro at micromolar concentration, thus providing a potential medical treatment for systemic anthrax infection. 4-Aminoquinolones are commonly used medicaments in the treatment of a variety of different diseases from malaria (chloroquine) to protozoal infection of the intestinal tract (quinacrine). Although it is still an open question if the channel lumen provides the pathway for the translocation of the enzymatic components, it could be shown for C2II that blockage of the channel inhibits in vivo intoxication of Vero cells (Bachmeyer et al., 2001). In this study, we provide evidence for the existence of one binding site inside the vestibule of the PA_{63}-channel for chloroquine, fluphenazine, and quinacrine. The binding kinetics of ligand binding to PA_{63} could be resolved by the ligand-induced current-noise analysis, resulting in on-rates that were dependent on the ionic strength of the aqueous phase and off-rates depending mainly on the structure of the ligand. The nonlinear relationship between single-channel conductance and KCl concentration and the high ligand affinity to PA_{63} at low ionic strength could be both explained by the existence of discrete negative charges inside the PA_{63}-channel.

REFERENCES

Andersen, C., M. Jordy, and R. Benz. 1995. Evaluation of the rate constants of sugar transport through maltoporin (LamB) of *Escherichia coli* from the sugar-induced current noise. *J. Gen. Physiol.* 105:385–401.

Bachmeyer, C., R. Benz, H. Barth, K. Aktories, M. Gilbert, and M. Popoff. 2001. Interaction of *Clostridium botulinum* C2-toxin with lipid bilayer membranes and vero cells: inhibition of channel function by chloroquine

and related compounds *in vitro* and intoxification *in vivo*. *FASEB J.* 15:1658–1660.

Bachmeyer, C., F. Orlik, H. Barth, K. Aktories, and R. Benz. 2003. C2-Rauschen mechanism of C2-toxin inhibition by fluphenazine and related compounds: investigation of their binding kinetics to the C2II-channel using the current noise analysis. *J. Mol. Biol.* 333:527–540.

Barth, H., D. Blocker, and K. Aktories. 2002. The uptake machinery of clostridial actin ADP-ribosylating toxins: a cell delivery system for fusion proteins and polypeptide drugs. *Naunyn Schmiedebergs Arch. Pharmacol.* 366:501–512.

Benz, R., K. Janko, W. Boos, and P. Läuger. 1978. Formation of large, ion-permeable membrane channels by the matrix protein (porin) of *Escherichia coli. Biochim. Biophys. Acta.* 511:305–319.

Benz, R., A. Schmid, and G. H. Vos-Scheperkeuter. 1987. Mechanism of sugar transport through the sugar-specific LamB channel of *Escherichia coli* outer membrane. *J. Membr. Biol.* 100:12–29.

Bezrukov, S. M., and M. Winterhalter. 2000. Examining noise sources at the single-molecule level: 1/f noise of an open maltoporin channel. *Phys. Rev. Lett.* 85:202–205.

Blaustein, R. O., and A. Finkelstein. 1990a. Voltage-dependent block of anthrax toxin channels in planar phospholipid bilayer membranes by symmetric tetra-alkylammonium ions. Effects on macroscopic conductance. *J. Gen. Physiol.* 96:905–919.

Blaustein, R. O., E. J. Lea, and A. Finkelstein. 1990b. Voltage-dependent block of anthrax toxin channels in planar phospholipid bilayer membranes by symmetric tetra-alkylammonium ions. Single-channel analysis. *J. Gen. Physiol.* 96:921–942.

Blaustein, R. O., T. M. Koehler, R. J. Collier, and A. Finkelstein. 1989. Anthrax toxin: channel-forming activity of protective antigen in planar phospholipid bilayers. *Proc. Natl. Acad. Sci. USA.* 86:2209–2213.

Blöcker, D., C. Bachmeyer, R. Benz, K. Aktories, and H. Barth. 2003. Channel formation by the binding component of *Clostridium botulinum* C2 toxin: glutamate 307 of C2II affects channel properties in vitro and pH-dependent C2I translocation in vivo. *Biochemistry.* 42:5368–5377.

Bradley, K. A., J. Mogridge, M. Mourez, R. J. Collier, and J. A. Young. 2001. Identification of the cellular receptor for anthrax toxin. *Nature.* 414:225–229.

Collier, R. J., and J. A. Young. 2003. Anthrax toxin. 2003. *Annu. Rev. Cell Dev. Biol.* 19:45–70.

Conti, F., and I. Wanke. 1975. Channel noise in membranes and lipid bilayers. *Q. Rev. Biophys.* 8:451–506.

Cunningham, K., D. B. Lacy, J. Mogridge, and R. J. Collier. 2002. Mapping the lethal factor and edema factor binding sites on oligomeric anthrax protective antigen. *Proc. Natl. Acad. Sci. USA.* 99:7049–7053.

Dani, J. A. 1986. Ion-channel entrances influence permeation. *Biophys. J.* 49:607–618.

De Felice, L. J. 1981. Introduction to Membrane Noise. Plenum Press, New York.

Dixon, T. C., M. Meselson, J. Guillemin, and P. C. Hanna. 1999. Anthrax. *N. Engl. J. Med.* 341:815–826.

Eigen, M., W. Kruse, G. Maass, and L. De Maeyer. 1964. Rate constants of protolytic reactions in aqueous solutions. *Prog. React. Kinet.* 2:287–318.

Elliott, J. L., J. Mogridge, and R. J. Collier. 2000. A quantitative study of the interactions of Bacillus anthracis edema factor and lethal factor with activated protective antigen. *Biochemistry.* 39:6706–6713.

Escuyer, V., and R. J. Collier. 1991. Anthrax protective antigen interacts with a specific receptor on the surface of CHO-K1 cells. *Infect. Immun.* 59:3381–3386.

Friedlander, A. M. 1986. Macrophages are sensitive to anthrax lethal toxin through an acid-dependent process. *J. Biol. Chem.* 261:7123–7126.

Hanna, P. C., D. Acosta, and R. J. Collier. 1993. On the role of macrophages in anthrax. *Proc. Natl. Acad. Sci. USA.* 90:10198–10201.

Jordan, P. C. 1987. How pore mouth charge distributions alter the permeability of transmembrane ionic channels. *Biophys. J.* 51:297–311.

Kobiler, D., Y. Gozes, H. Rosenberg, D. Marcus, S. Reuveny, and Z. Altboum. 2002. Efficiency of protection of guinea pigs against infection with *Bacillus anthracis* spores by passive immunization. *Infect. Immun.* 70:544–560.

Lacy, D. B., and R. J. Collier. 2002. Structure and function of anthrax toxin. *Curr. Top. Microbiol. Immunol.* 271:61–85.

Little, S. F., B. E. Ivins, P. F. Fellows, and A. M. Friedlander. 1997. Passive protection by polyclonal antibodies against *Bacillus anthracis* infection in guinea pigs. *Infect. Immun.* 65:5171–5175.

MacKinnon, R., R. Latorre, and C. Miller. 1989. Role of surface electrostatics in the operation of a high-conductance Ca^{2+}-activated K^+ channel. *Biochemistry.* 28:8092–8099.

Menard, A., K. Altendorf, D. Breves, M. Mock, and C. Montecucco. 1996. The vacuolar ATPase proton pump is required for the cytotoxicity of Bacillus anthracis lethal toxin. *FEBS Lett.* 386:161–164.

Mock, M., and A. Fouet. 2001. Anthrax. *Annu. Rev. Microbiol.* 55:647–671.

Mourez, M., R. S. Kane, J. Mogridge, S. Metallo, P. Deschatelets, B. R. Sellman, G. M. Whitesides, and R. J. Collier. 2001. Designing a polyvalent inhibitor of anthrax toxin. *Nat. Biotechnol.* 19:958–961.

Nassi, S., R. J. Collier, and A. Finkelstein. 2002. PA_{63} channel of anthrax toxin: an extended beta-barrel. *Biochemistry.* 41:1445–1450.

Nekolla, S., C. Andersen, and R. Benz. 1994. Noise analysis of ion current through the open and the sugar-induced closed state of the LamB-channel of *Escherichia coli* outer membrane: evaluation of the sugar binding kinetics to the channel interior. *Biophys. J.* 86:1388–1397.

Nelson, A. P., and D. A. McQuarrie. 1975. The effect of discrete charges on the electrical properties of a membrane. *J. Theor. Biol.* 55:13–27.

Orlik, F., C. Andersen, and R. Benz. 2002. Site-directed mutagenesis of tyrosine 118 within the central constriction site of the LamB (maltoporin) channel of Escherichia coli. II. Effect on maltose and maltooligosaccharide binding kinetics. *Biophys. J.* 83:309–321.

Orlik, F., C. Andersen, C. Danelon, M. Winterhalter, M. Pajatsch, A. Böck, and R. Benz. 2003. CymA of *Klebsiella oxytoca* outer membrane: binding of cyclodextrins and study of the current noise of the open channel. *Biophys. J.* 85:876–885.

Pellizzari, R., C. Guidi-Rontani, G. Vitale, M. Mock, and C. Montecucco. 1999. Anthrax lethal factor cleaves MKK3 in macrophages and inhibits the LPS/IFN gamma-induced release of NO and TNF alpha. *FEBS Lett.* 462:199–204.

Petosa, C., R. J. Collier, K. R. Klimpel, S. H. Leppla, and R. C. Liddington. 1997. Crystal structure of the anthrax toxin protective antigen. *Nature.* 385:833–838.

Sellman, B. R., M. Mourez, and R. J. Collier. 2001a. Dominant-negative mutants of a toxin subunit: an approach to therapy of anthrax. *Science.* 292:695–697.

Sellman, B. R., S. Nassi, and R. J. Collier. 2001b. Point mutations in anthrax protective antigen that block translocation. *J. Biol. Chem.* 276:8371–8376.

Song, L., M. R. Hobaugh, C. Shustak, S. Cheley, H. Bayley, and J. E. Gouaux. 1996. Structure of staphylococcal alpha-hemolysin, a heptameric transmembrane pore. *Science.* 274:1859–1866.

Verveen, A. A., and L. J. De Felice. 1974. Membrane noise. *Prog. Biophys. Mol. Biol.* 28:189–265.

Wohnsland, F., and R. Benz. 1997. 1/*f*-Noise of open bacterial porin channels. *J. Membr. Biol.* 158:77–85.